PHYSICAL REVIEW B VOLUME 21, NUMBER 12 15 JUNE 1980

Molecular structure of As_2Se_3 glass

J. C. Phillips
Bell Laboratories, Murray Hill, New Jersey 07974

C. Arnold Beevers and S. E. B. Gould
Department of Chemistry, University of Edinburgh, Edinburgh, EH9 3JJ, Scotland

(Received 26 July 1979)

Molecular models are constructed for large structural units appropriate to $As_xS_{1-x}(Se_{1-x})$ glasses near $x = 0.4$. The models are similar to those previously constructed for $Ge_yS_{1-y}(Se_{1-y})$ glasses near $y = 0.33$. Comparison of the models explains anomalies in the temperature and pseudobinary alloying dependence of diffraction data. Anomalies in the Raman scattering from local vibrational modes, particularly at low frequencies, are also resolved by the models. As a byproduct, the model explains the bimodal quadrupolar asymmetry of $AsSe_3$ pyramidal glass units.

I. INTRODUCTION

The chalcogenide alloys $Ge_x(As_x)S_{1-x}(Se_{1-x})$ form solid solutions over a wide composition range and for appropriate x can be cooled very slowly (at rates as low as 10^{-6} K/sec) to form glasses. A close connection exists in these materials between the microscopic chemical bonds and the favorable glass-forming tendencies. Because the bonding is predominantly covalent one of us was able to demonstrate an algebraic topological relationship between composition and glass-forming tendency; this relationship is in excellent agreement with experiment.[1] According to this relationship, when the $8-N$ rule for nearest-neighbor coordination and cation-anion alternation (chemical ordering) are satisfied, the glass-forming tendency is greatest when the short-range order imposed by bond stretching and bending forces is just sufficient to exhaust local degrees of freedom; i.e., the short-range configurational entropy and strain energy are nearly zero.

An immediate implication of this model (called the valence force-field constraint theory) is that near the composition which maximizes the glass-forming tendency substantial medium-range order is expected in not only the glass ($T < T_g$) but also the supercooled liquid ($T_g < T < T_m$) and even the normal liquid ($T_m < T$). This order is observable through anomalies in microscopic properties such as x-ray diffraction and Raman-active vibrational modes, as well as macroscopic properties (photo and acoustic fatigue, for example).

The first observation of a microscopic anomaly in these materials was the discovery[2] of a first sharp diffraction peak in $g-As_2Se_3$. Similar peaks have since been reported in many covalent materials with mean coordination numbers between 2.3 and 3.0. In a few cases (notably As_xS_{1-x} films prepared by evaporation) this peak is identified with the spacing of spheroidal clusters (i.e., As_4S_4) which are stable as free molecules; annealing of such films reduces the peak intensity and suggests that the clusters exist in the glass as artifacts of the preparative procedure. However, as one of us has reviewed elsewhere,[3] in most cases the first sharp diffraction peak in the glass measures the spacing of layered molecular clusters, and this spacing at low temperatures agrees well with the interlayer spacing in the corresponding crystal, e.g., $c-As_2Se_3$ or $c-GeSe_2$.

At this point one may propose that the observed anomaly arises from the presence of microcrystallites in the glass; from the width of the first sharp diffraction peak one can then infer that the smallest such microcrystallites are 15–30 Å in diameter. This explanation is inadequate, however, because the diffraction anomaly has been observed[4] for both $GeSe_2$ and As_2Se_3 in the *normal* liquid, i.e., for $T > T_m$. Because the crystal and the normal liquid are separated by a first-order phase transition, the "microcrystallite" theory[2] cannot be used to justify the presence in the normal liquid of molecular clusters containing several hundred atoms. Another objection to the microcrystallite model is the observation in $g-GeS_2(Se_2)$ of a companion A_1 Raman line, second in intensity only to the A_1 [symmetric breathing mode of $Ge(S_{1/2})_4$ tetrahedra] line itself. This line is completely absent from the crystalline Raman spectrum.

In the case of $g-GeS_2(Se_2)$ these puzzles have recently been resolved by the construction of a specific model of a large molecular cluster which has a layer structure very similar to that of the crystal (in its high-temperature form) but which is terminated in a characteristic manner which accounts for the companion Raman line.[5] The topologically significant features of this cluster (which is called an "outrigger raft") are reviewed in Sec. II; they

are invaluable as a guide for our analysis of As_2Se_3 molecular clusters. In Sec. III we review the crystal structure of As_2Se_3 (orpiment) in order to identify the structural subunits which may (or may not) be transferred to the large glass clusters. The remaining sections utilize data on the pseudobinary[6] and temperature[4] dependence of the first sharp diffraction peak to construct a plausible model of the molecular structure of g–As_2Se_3.

The central conclusion of our analysis is that the molecular clusters in g–As_2Se_3 are rafts like the raft in $GeSe_2$. However, in $GeSe_2$ the structure of the raft is conformationally unique, while in As_2Se_3 there are at least four distinct conformers whose statistical weight varies with pseudobinary alloying and temperature. These conformers exist because the local enantiomorphic balance of $As(Se_{1/2})_3$ units in the crystal is weakly broken in the glass.

When the disordered solid contains microcrystallites or only one distinct conformer (as in $GeSe_2$) then we have, in effect, structurally equivalent nucleation centers for crystallization, and it may be very difficult to anneal through the glass transition (at $T = T_g$) without first crystallizing the material. On the other hand, the existence of a large number of distinct conformers in supercooled liquid $As_2S_3(Se_3)$ helps to explain why single crystals of these materials can be grown only very slowly, and why the glass-forming tendency of $As_xS_{1-x}(Se_{1-x})$ alloys can be so pronounced even at the crystalline composition $x = 0.4$.

The remainder of the paper reviews the evidence for our model. Some suggestions are made in the concluding section for Raman scattering experiments on pseudobinary alloys that might test the proposed model.

II. OUTRIGGER RAFTS IN $GeS_2(Se_2)$

Because corner-sharing chalcogen bond angles in $GeS_2(Se_2)$ are about 100°, which is close to 90°, the A_1 symmetric tetrahedral breathing modes are decoupled and the A_1 Raman line is very narrow [$\nu_{1/2}(\mathrm{FWHM})/\nu = 0.015$] as is its companion.[5] These two glass lines are by far the narrowest ones known which are localized on clusters which form the main covalent network (and are not, e.g., additive elements) of the noncrystalline material. Because the dependence on composition $I_c(y)$ of the companion line in $Ge_yS_{1-y}(Se_{1-y})$ glasses is so great [$I_c(y) \propto y^5$ for $0 \leq y \leq \frac{1}{3}$] we know that molecular clusters containing at least five formula units must be responsible for the line. By comparing the isotopic shifts from GeS_2 to $GeSe_2$ we also know that the companion line must be associated primarily with chalcogen motion. However, the companion line cannot be explained by another network tetrahedral mode, e.g., edge-sharing (instead of corner-sharing) tetrahedra because both of these modes are resolved in the crystalline spectra and their splitting is too small to account for the observed splitting of the A_1 and companion lines in the glass.

A resolution of this problem, which has puzzled many workers over a period of nearly a decade, is shown in Fig. 1. A raft is constructed which is similar to the layer structure of the crystal. Normal to the layer or raft plane the sheets are only van der Waals (not covalently) bonded, a situation which is described here as monomerization (decoupling) in one coordinate. The raft, however, has been monomerized in a second (here along the b axis) coordinate by selective removal of Ge atoms and rebonding (dimerization) of edge chalcogens. The rafts are still polymerized along the a axis, as indicated by the dashed lines. Thus the rafts are polymerized along one coordinate and monomerized along the other two, which is equivalent topologically to the situation for Se (and various polymeric) chains. Finally, the radial breathing modes (in-phase) of the dimerized chalcogens can readily account for the narrow companion Raman line.

It is quite possible that the topological properties of the outrigger raft, i.e., linear polymerization along only one coordinate, are very favorable to

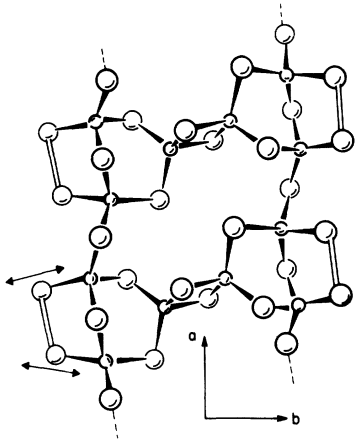

FIG. 1. The large clusters which are the dominant structural elements of glassy $GeSe_2$ are supposed to be made of stacked layer units of the kind shown here. The chalcogen atoms on the edges of the units have dimerized, while the chalcogen atoms at the ends of the chains reconstruct in some other manner, e.g., in an Se-rich environment they may polymerize with Se chains. Note the edge-sharing tetrahedra which stabilize the double-chain structure. The companion Raman line is associated with coupled motion of the dimerized chalcogens, as indicated by the double arrows. The chains run parallel to the a axis.

glass formation. (It was previously shown[1] that the number of degrees N_d of freedom per atom, i.e., the dimensionality of the space in which the material is embedded, play a central role in determining the glass-forming tendency as a function of composition in these alloys.) It is easy to see that linear polymers can be packed efficiently to form bundles, while if the raft in Fig. 1 could somehow be bordered along two adjacent edges with chalcogens and polymerized along the other two, steric hindrances would be likely to develop in this bent conformation which would ultimately increase the internal energy of the supercooled liquid by so much as to facilitate recrystallization. We therefore assume in what follows that linear polymerization lowers the internal energy of packed rafts more than, e.g., bent conformations would, and confine ourselves to raft conformers of the linear kind.

III. THE STRUCTURAL ELEMENTS OF ORPIMENT

The layer structure of orpiment is illustrated in Fig. 2. At first sight the layers appear to consist of zigzag, almost trigonally equivalent chains. However, the five atoms per formula unit are structurally inequivalent.[7] The structure of As_2Se_3 actually consists of As(1)–Se(1)–As(2)–Se(2) spiral chains cross linked by Se(3). Intrachain Se(1, 2) angles are close to 100° while the interchain Se(3) angle is close to 85°. This is a large difference, comparable to the difference of corner-sharing (100°) Se atoms compared to edge-sharing (80°) Se atoms in the $GeSe_2$ layer structure. This difference in the $GeSe_2$ crystal is preserved in the g–$GeSe_2$ raft shown in Fig. 1 and we might well expect the Se(1, 2) Se(3) bond-angle difference in orpiment to be transferred to rafts in g–As_2Se_3. The Se(3) atoms lie near the center of each layer, the Se(1) and Se(2) atoms near the surface, and the As(1) and As(2) atoms between the Se(1), Se(3), and Se(2) layers, respectively. Thus the orpiment

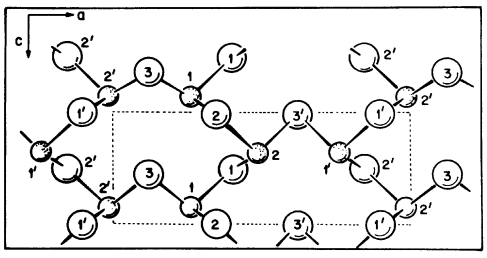

FIG. 2. A perspective view of the orpiment structure, with the atoms labeled for reference and comparison with the rafts illustrated in subsequent figures. The orpiment chains As(1)–Se(1)–As(2)–Se(2) (and similarly for the primed enantiomorph) run vertically. The dashed lines indicate the planar unit cell.

structure is really a five-layer structure, in contrast to layer $GeSe_2$ which is trilayer.

The second structural element of importance is the difference between As(1, 2) $(Se_{1/2})_3$ clusters; the bond angles around As(1) span a narrow range of 9°, while the As(2) bond angles span the much wider range of 13°. The As(1) and As(2) atoms alternate around the As_6Se_6 ring which is the smallest ring in the layer structure. It appears that this alternation facilitates the simultaneous formation of the layer structure and the (relatively) compact rings. To the extent that both these features are present in the glassy raft we would expect the distinction between and alternation of As(1) and As(2) to be transferred to the raft rings as well.

There is a third symmetry element in the crystal structure which is more subtle. Each As atom has a blind side, with the $(Se_{1/2})_3$, say, all having $\xi > 0$ and $\xi(As) = 0$. Looking along the ξ axis, and numbering the Se atoms clockwise, the largest (α) and smallest (β) Se–As–Se angles are Se(1)–As(1)–Se(3) and Se(2)– As(1)–Se(3) for As(1); these roles are reversed for As(2). The foregoing construction describes the As atoms on one spiral chain. The As(1′, 2′) atoms on the adjacent spiral chain are enantiomorphic images of As(1, 2); i.e., they have the same respective structures but the $(Se_{1/2})_3$ atoms all lie on the $\xi < 0$ side. Now an As_6Se_6 ring consists of two adjacent chain segments As_3Se_2 and $As_3(')Se_2$ with ends cross-linked by two Se(3) atoms. Thus each ring is enantiomorphically balanced, with equal numbers of primed and unprimed As atoms. It is quite possible that enantiomorphic balance is not a necessary feature in a glassy raft.

IV. ORPIMENTAL RAFTS

To construct rafts with structures close to that of the crystal, we have selected the basic ring As_6Se_6 of orpiment and polymerized it at two opposite ends with $(Se_{1/2})_2$ while bordering it on two opposite sides with Se_3 (Se–Se–Se bond angle 104°, as in crystalline Se) outrigger units (cf. Fig. 1). The outrigger units contain (of necessity) an extra bridging Se atom each, and the formula for each cluster is $(As_2Se_3)_3Se_3(Se_{1/2})_2$; the stoichiometry As_xSe_{1-x} is close to $x = 0.3$ instead of 0.4. However, polycyclic rafts can be constructed for g–As_2Se_3 by using several orpimental rings, continued parallel to the a axis in Fig. 2, or for g–$GeSe_2$ by using several double chains parallel to the b axis in Fig. 1, and finally bordering each raft with chalcogen outrigger units. This will bring the stoichiometry closer to the ideal values (which maximize T_g) of $x = 0.4$ and $y = 0.33$ for As_xSe_{1-x} and Ge_ySe_{1-y} alloys,

respectively. Smaller cation-rich molecules, such as As_4Se_4 or $Ge_2(Se_{1/2})_6$, can also be used to correct the stoichiometry through association with chalcogen-bordered rafts. The nonlinear shift in $T_g(x)$ from $x=0.3$ to 0.4 is small ($\lesssim 40°$) which is consistent with the energies of association of larger molecules. Finally, we note that many properties of $(GeSe_2)_{1-x}(As_2Se_3)_x$ alloys [such as the composition dependence of the intensity $I_c(x)$ of the companion Raman line] are very similar to those of $(GeSe_2)_{1-x}(Se_5)_x$ alloys.[5] This suggests that the basic As–Se and Ge–Se clusters have linear polymerized structures similar to that of Se chains, so that parallel bundles can be formed in all cases.

The construction of models is greatly facilitated by the availability of standard orpiment model kits which have been designed by one of the authors. In these kits the atoms are labelled As(1, 2) or Se(1, 2, 3) and may also be primed enantiomorphs or not. With these prepared atoms it would appear to be easy to construct a large number of distinct conformers, but the requirement of closure of the raft (except for the polymerized $Se_{1/2}$ atoms at opposite ends of the ring) is severely restrictive. In fact, we have tried to construct rafts by violating one of the rules described in Sec. III. In five out of six cases closure was not achieved. In the one case where it was achieved, one of the outrigger units was so severely deformed as to be re-entrant in a projection on the plane of the raft. We have constructed four conformer rafts which we believe explain adequately certain features of the experimental data discussed in subsequent sections; all of these meet the requirements described in Sec. III.

We are aware, of course, that many other rafts containing 20 or more atoms can be constructed, so that our models are by no means unique. Their significance lies in the comparison with the $AB_2 = GeSe_2$ raft (based on coordination numbers $N_A=4$, $N_B=2$) and the differences that arise because for A_2B_3 we have $N_A=3$ and $N_B=2$. The mean coordination numbers in these two kinds of rafts are quite similar, but the mean square coordination numbers differ more significantly. Thus, as previously discussed,[1] the topological constraints on AB_2 rafts are much more restrictive than for A_2B_3 rafts. The topological argument[1] envisioned an infinite, undifferentiated (i.e., three-dimensional) covalent network whereas our models

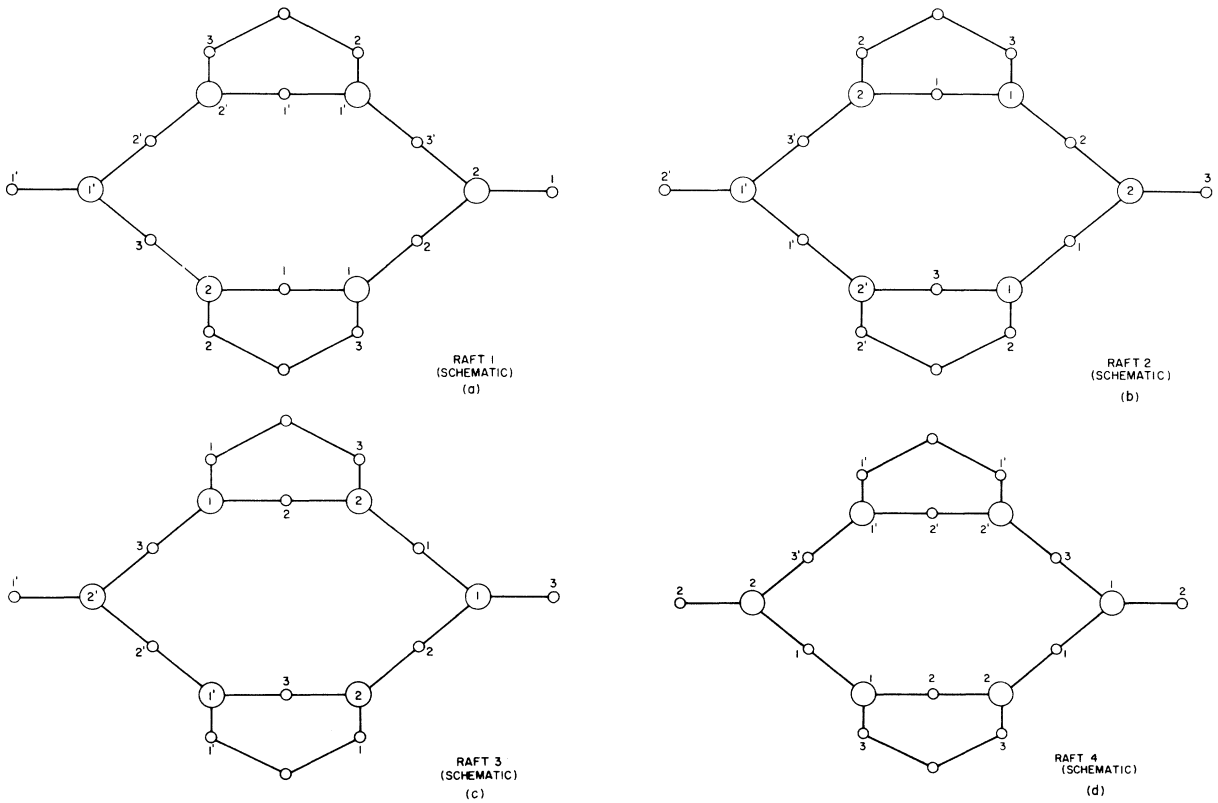

FIG. 3. Schematic diagram of orpimental rafts. The conformer configurations of the "outrigger" sections can have either the "boat" or "chair" forms. Where possible the "chair" form has been used in constructing the models, as in organic molecules the "chair" form is usually energetically preferred.

have layer structures and contain only about 20 atoms. It was previously suggested[1] that in good glasses cluster effects were of secondary importance compared to network effects, and it is certainly plausible that this should be the case when the clusters contain so many atoms. Our models confirm this reasoning, but they also make it possible for us to discuss several features of the experimental data—especially the first sharp diffraction peak which is associated with the interlayer spacing—which were not accessible to the more abstract and less specific argument.

The four conformer rafts, all of which satisfy the rules of the preceding section, are shown schematically in Fig. 3. Raft 1 is formed from enantiomorphically balanced chain segments, $As_3(1,2)$ and $As_3(1',2',)$, and it has symmetry C_{2v}. This is the only symmetric raft and it is directly comparable to the $GeSe_2$ raft shown in Fig. 1. A perspective drawing of raft 4 is shown in Fig. 4.

Rafts 2–4 contain either two As(1′, 2′,) and four As(1, 2) or the reverse; they are enantiomorphically weakly imbalanced (weakly broken enantiomorphic symmetry). The minority As(1′, 2′,) atoms can include an end atom (rafts 2 and 3) or can be both border atoms (raft 4). In raft 2 (3) the minority end atom is 1′ (2′). We have constructed models of raft 2 with both outrigger units in the "boat" conformation (2B) [Fig. 3(b)] or the "chair" conformation (2C) [Fig. 3(b)].

The spacings normal to the layers of the extreme atom positions in each raft are $\delta = 2.90$, 3.48, 3.77, 3.77, and 4.06 Å for rafts 1, 2B, 2C, 3 and 4, respectively, compared to $\delta = 2.90$ Å in orpiment itself. (The raft spacings are probably accurate only to 5%.) Note the gap in the distribution of δ between raft 1 (enantiomorphically balanced) and the remaining imbalanced structures. These spacings will be used in the following section to estimate the dependence on conformer type of the mean inter-raft spacing d.

V. INTERLAYER ADAPTABILITY: PHYSICAL ORIGIN OF S_c

In order to discuss thermal and chemical trends of the first sharp diffraction peak in the layer model we need a general, qualitative description of the interactions responsible for the interlayer spacing $S_c = 2\pi/k_c$. In crystals (where the atomic structure is known accurately) the interlayer spacing d can be said to be determined by the van der Waals interactions between pairs of chalcogens on adjacent layers which approach each most closely (compared to other similar pairs). How can this description be extended to the more general situation of stacked, conformerically variable rafts in liquids and glasses?

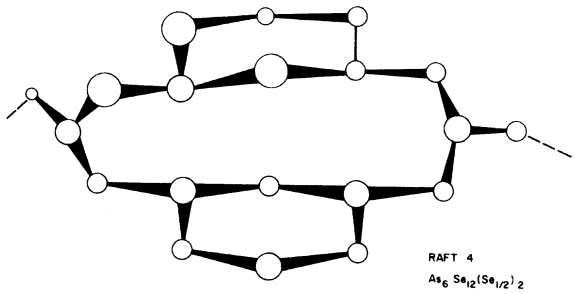

FIG. 4. Perspective drawing of rafts 4.

First we notice that the van der Waals interaction contains both a long-range attractive component (due to mutually induced virtual polarizations of the interacting layers) and a short-range repulsive component (exclusion principle or Fermi repulsion) from lone pairs. Thus, the layers are free to slide or rotate relative to one another in order to maximize the former while still maintaining the minimum distance of closest nonbonded interatomic approach D_0 implied by the very rapid (exponential) increase of the latter interaction for interlayer spacing D of order D_0.

Our problem now is to construct a model which takes account of the sliding and rotational degrees of freedom available to stacked layers as they adjust their configurations to optimize the van der Waals interaction. This is the problem of interlayer adaptability. In general we would expect the solution to this problem to involve both the van der Waals radii D_0 and the layer corrugation amplitude δ, defined as the center-to-center spacing of the extremal atoms of a given unit.

Now in the limit of planar layers (such as graphite) by definition $D = D_0$. This suggests that for $\delta/D_0 \ll 1$ we might add to this relation a correction of order $(\delta/D_0)^n$, where $n > 2$ is a dimensionless adaptability index. (The choice $n = 2$ corresponds to a kind of randomness in the adaptability.) The limit $\delta/D_0 \gg 1$ describes a structure which no longer has a truly layer or two-dimensional character. Unfortunately, the actual values of δ/D_0 for A_2B_3 and AB_2 layer crystals[7,8] are of order 0.7–0.9, and several of the orpimental rafts described in the previous section correspond to $\delta/D_0 = 1.0$, which may well represent the limit of raft stability. The proposed correction term does not seem appropriate for such large values of δ/D_0, and an analytic formula which reduces to the van der Waals limit as $\delta/D_0 \to 0$ seems to have little value.

If we compare the crystalline values of δ/d with d/D_0 [where $D_0 = 3.7$ Å(S) or 4.0 Å(Se), either from the interlayer distances of closest B-B approaches, or from Pauling[9]], then we find little correlation

of d with D_0 in terms of chemical shifts in B (same crystal structure). Thus the 8% increase in D_0 from B = S to B = Se produces a 4% increase in $d(As_2B_3)$ and a 3% increase in $d(GeB_2)$. We conclude that the competition between the interlayer van der Waals forces and the intralayer bond-bending forces (which determine the corrugation amplitude δ) is quite complex. In particular, the former increase with increasing core size, while the latter decrease. (This latter effect is sometimes called[10] "metallization.")

If we compare the crystalline values[7,8] of δ/d, we discover a remarkable fact: $\delta/d = 0.28$ for As_2S_3 and GeS_2, and $\delta/d = 0.30$ for As_2Se_3 and $GeSe_2$. Thus the simplest and probably most reliable description is

$$\delta = (0.29 \pm 0.01)D \qquad (1)$$

for the rafts as well. This formula is surprising because it does not contain the van der Waals spacing D_0 at all, even though the van der Waals interaction geometrically determines the actual atomic interlayer distance of closest approach.

Suppose we have a range of values of δ derived from conformer rafts in the glass. The rafts form stacks, with the normal to each raft in the stack nearly parallel to the stack normal. Again because of van der Waals forces there will be adjacent stacks with nearly parallel normals. Adjacent stacks will tend to match chalcogenide-bordered (nonbonded) edges and these edges will tend to be staggered between rafts belonging to adjacent stacks. Because the second derivative of the repulsive part of the van der Waals interaction is much larger in magnitude than the second derivative of the attractive part, the larger values of δ will be weighted more heavily than the smaller ones by the interactions between adjacent stacks. The same interaction can also cause the observed distribution to appear to be much narrower than would be predicted by the intrinsic population distribution of conformers. Thus at high temperatures the intrinsic population distribution of conformers might be nearly uniform, but because of the interstack interactions the larger values of δ will dominate, and the observed peak width of S_c will be narrow.

VI. TEMPERATURE DEPENDENCE OF THE FIRST SHARP DIFFRACTION PEAK

One of the controversial questions in the atomic structure of chalcogenide glasses such as g–As_2Se_3 and g–$GeSe_2$ has been the degree to which the short- and medium-range order can be described as microcrystalline.[2,11] The decisive experiment on this question has recently been presented by neutron diffraction not only from the solid ($T < T_g$) and the supercooled liquid ($T_g < T < T_m$) but also the normal liquids ($T > T_m$) of these materials.[4] These data are reproduced, for the reader's convenience, in Fig. 5 for $GeSe_2$ and in Fig. 6 for As_2Se_3.

The following features of the data are noteworthy: At $T = 771$ C $> T_m(GeSe_2) = 740$ C the anomalous FSDP (first sharp diffraction peak) near $k = k_c = 1.0$ Å^{-1} is still present (hence no microcrystallites). It is broadened slightly but is shifted from the solid value by less than 5%. Much more dramatic are the data for As_2Se_3 shown in Fig. 6. In reduced temperature units $Z = T/T_m$, the range of temperature is much greater [$T_m(As_2Se_3) = 380$ C = 650 K, $Z = 0.4$ to 1.4]. Dramatic changes are observed in the FSDP over this temperature range. At $Z = 1.25$, $k_c = 1.2$ Å^{-1}, at $Z = 1.03$ it has shifted to $k_c = 1.3$ Å^{-1}. At $Z = 0.4$ ($T < T_g = 170$ C) the glassy first diffraction peak is no longer sharp. Perhaps a second peak has started to form near $k = 1.7$ Å^{-1}, but in any case k_c appears to have shifted to about 1.5 Å^{-1}.

These phenomena can be explained quite simply by the raft models we have discussed. The $GeSe_2$ conformer raft, Fig. 1, is unique, so the stability of $k_c(T)$ in position should persist as long as the FSDP exists. We have exhibited four different conformer rafts for As_2Se_3. At high temperatures these may be present in approximately equal numbers, but, as noted in Sec. V, k_c in this case is determined primarily by the most highly corrugated rafts. At low T only the most symmetric rafts with values of δ close to the crystalline value δ_0, may be present in large numbers. Thus the appar-

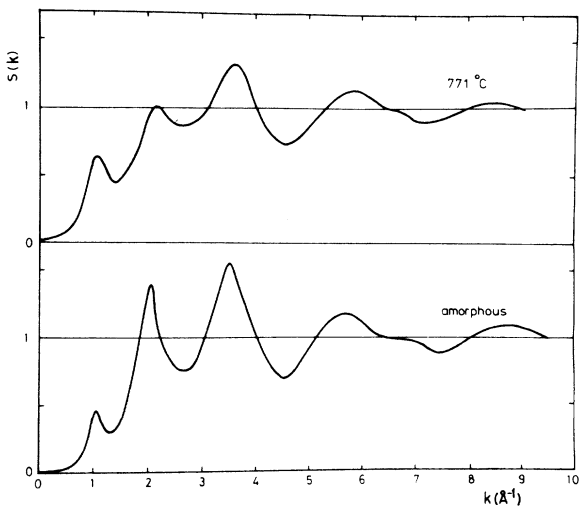

FIG. 5. The structure factors $S(k)$ for glassy (amorphous) $GeSe_2$ and for liquid ($T = 771$ C $> T_m$) $GeSe_2$. The feature of greatest interest is the first sharp diffraction peak (FSDP) near $k = 1.0$ Å^{-1}. Data from Ref. 4.

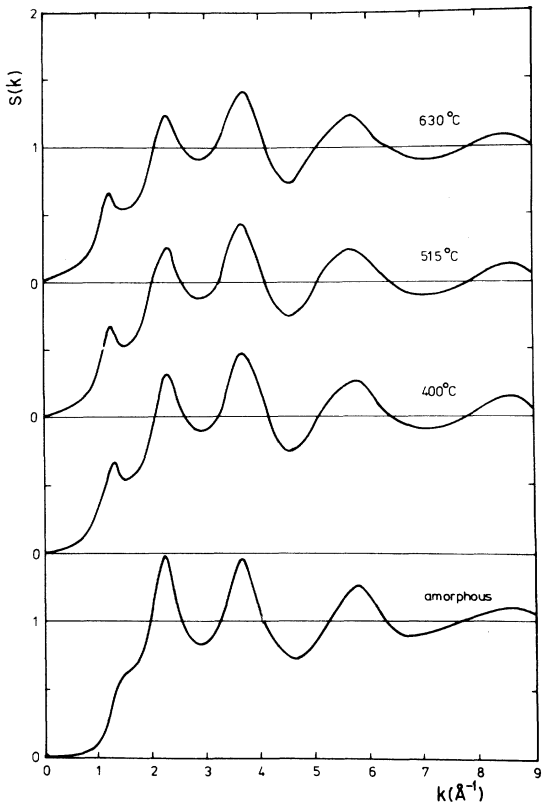

FIG. 6. The structure factors $S(k)$ for glassy (amorphous) As_2Se_3 and liquid As_2Se_3 (T_m = 380 C). Data from Ref. 4.

ent value of δ is much reduced and k_c should increase with decreasing T, as observed. The range spanned by δ among the four rafts is $\delta_0 \lesssim \delta \lesssim 1.4\delta_0$, so that the shift in k_c of about 25% is quite consistent with the model values, especially when allowance is made for the weighting of larger values of δ at higher T by interstack interactions.

In the glassy (or amorphous) sample shown in Fig. 6 we noticed that there was evidence for a second peak, or at least a second mechanism which broadens the first diffraction peak relative to its high-T value. In discussing raft structures we recognized two factors, chalcogenide bordering along one set of parallel edges, and polymerization of the other set. At high T the staggering of bordered edges of adjacent stacks may be the dominant interstack interaction, but at low $T \lesssim T_g$ the polymerizing interactions may be also significant. Now the latter tend to *align* (rather than stagger) rafts from adjacent stacks (probably through three-stack interactions), and this would give closer packing (and a high-k shoulder on the FSDP). Some of the chalcogen borders may also react, e.g., with As-rich molecules (such as As_4Se_4) to increase the lateral extent of a raft so that it more nearly resembles a fragment of a crystalline layer. While this explanation is only tentative, it contains an interesting paradox: the initial signature of the nucleation of microcrystallites could be a *broadening* of the FSDP.

VII. PSEUDOBINARY ALLOYS

One of the paradoxes discussed in the preceding section was the fact that reduction of T in As_2Se_3 broadened (rather than narrowed, as one would ordinarily have expected) the FSDP. In pseudobinary alloys $As_2Se_mTe_{3-m}$ one would expect that the narrowest FSDP would be found for $m = 0$ or 3, but just the opposite is the case. Here the data,[6] taken by electron diffraction, are again reproduced for the reader's convenience in Fig. 7. The order of the peak widths Γ_m is $\Gamma_1 \lesssim \Gamma_2 \ll \Gamma_3 < \Gamma_0$. The broad peak in g-As_2Te_3 is expected, because c-As_2Te_3 does not have a layer structure.[1]

To understand why Γ_1 and Γ_2 are so small, we examine the rafts as well as the c-As_2Se_3 structure. In most cases we find a tendency towards a five-layer structure Se–As–Se–As–Se. Thus $m = 2$ and 1 could correspond to Se–As–Te–As–Se and Te–As–Se–As–Te, respectively. The latter layering is particularly attractive, because the larger, less covalent Te atoms form the outside layers, and indeed the data seem to suggest $\Gamma_1 < \Gamma_2$.

In general the achievement of cation or anion subsite segregation in covalent networks is greatly hindered in crystals by strain energies, unless the latter can be relieved by a phase transition to a lower symmetry. Thus in the chalcopyrite structure ($A^{N-1}B^{N+1}C_2^{8-N}$) the cubic zinc-blende structure becomes tetragonal when the A and B cations

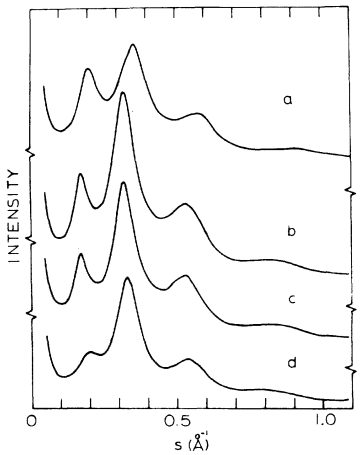

FIG. 7. Diffracted electron intensity as a function of scattered wave vector s for four alloys, a, b, c, d, corresponding respectively to $m = 0$, 1, 2, 3 in $As_2Se_{3-m}Te_m$. The FSDP is located near $s = 0.2$ Å^{-1}. Data from Ref. 6.

order in planes.[12] In solid electrolytes based on AgI and Cu halides, where the lowest optic phonon frequencies[13] are also of order 20 cm^{-1} (similar to $GeSe_2$ and As_2Se_3), anion site segregation has recently been achieved[14] in $RbCu_4I_2Cl_3$, but the "liquidity" of the Cu cations here acts to reduce the strain energies. Attempts to achieve anion site segregation (differentiating intrachain and interchain sites) in As_2Se_2S crystals have apparently failed.[15] This makes the possibility of site segregation in g–As_2Te_2Se rafts of great interest.

The alloy data in Fig. 7 are informative and support the layer model but they do not provide a decisive *test* of the raft model *per se*. We now discuss an experiment which should contain additional (and perhaps more conclusive) evidence.

VIII. RAMAN SCATTERING: LOW-FREQUENCY PHONONS AT LOW T

One of the characteristic features of layer structures is the presence of very low-frequency optic modes associated with interlayer vibrations which involve only van der Waals restoring forces. The Raman scattering spectra at room temperature have been reported for c–$As_2(S, Se)_3$ using an He–Ne laser.[16] The interlayer phonons definitely are represented by a strong line at (25, 21) cm^{-1} and by a weaker line at (36, 32) cm^{-1}. With a Kr^+ laser a strong line at 30 cm^{-1} and a medium line at 17 cm^{-1} have been observed at room temperature in $GeSe_2$ crystals.[5]

Low-temperature ($T \sim 10$ K) Raman scattering[17] from g–$As_2(S, Se)_3$ and g–$Ge(S, Se)_2$ has shown a characteristic shoulder at low frequencies followed by a slowly decreasing plateau. The positions of the shoulders are 25, 20, 22, and 17 cm^{-1}, respectively. The positions of the first optic phonons in c–$As_2(S, Se)_3$ and c–$GeSe_2$ agree well with the positions of the shoulders. At room temperature in g–$GeSe_2$ a broadened peak is observed[5] centered near 29 cm^{-1}, again in good agreement with c–$GeSe_2$. The second peak was not observed either in g–$As_2(S, Se)_3$ or g–$Ge(S, Se)_2$ in the low-temperature data[17] taken on polished samples, presumably because of surface damage which disrupted the orientation of the stacked rafts. It would be of considerable interest to study Raman scattering at low T from virgin surfaces of these materials; we expect that both interlayer optic phonons would then be easily resolved.

In Sec. VI we saw that electron-diffraction data on $As_2Se_mTe_{3-m}$ alloys indicate segregation of Se and Te in a pentalayer structure, accompanied by a sharpening of the interlayer spacing. This should produce optic phonon multiplets in Raman scattering from virgin glass samples at low T using gas lasers. Again experiments of this kind should be structurally revealing.

IX. POSTSCRIPT

After completion of this article measurement of the electric-field-gradient ellipsoidal asymmetry parameters of pyramidal AsB_3 units in g–As_2Te_3 was reported.[18] The experimental results are very well explained by the outrigger raft model as follows.

In c–As_2Se_3 (orpiment) there are two values[19] of $\eta = (q_{XX} - q_{YY})/q_{ZZ}$ (q_{IJ} is the quadrupole coupling tensor), $\eta = 0.34$ and 0.37, corresponding to the As(1) and As(2) pyramidal units. In g–As_2Se_3 again two values are found $\eta_1 = 0.14$ (width 0.07, weight 0.6) and $\eta_2 = 0.45$ (width 0.14, weight 0.4). According to the outrigger raft model, in each As_6Se_6 orpimental ring, there are four As atoms connected to outrigger units and two As atoms at opposite ends of the raft which are polymerized (through Se atoms) to the rest of the (predominantly chemically ordered) covalent network. The η_1 component of the asymmetry is assigned to the four outrigger atoms (weight 0.67), while the η_2 component is assigned to the two end atoms (weight 0.33).

The values of η_1 and η_2 can be understood by noting that the number of VFF constraints near the outrigger units is much lower than average because of the presence of the additional B = 2 chalcogen atoms. This permits greater relaxation[20] of the outrigger As pyramidal units towards cylindrical symmetry ($\eta = 0$) because one of the As *second* neighbors is an underconstrained chalcogen. On the other hand, the value of η_2 (end atoms) should be substantially the same as η (crystal), and this is the case within the limits of the experimental uncertainties. It is remarkable that the outrigger structure has now been identified specifically in the closely related materials g–$GeSe_2$ and g–As_2Se_3 through two completely unrelated experiments, viz., the companion Raman line in the former[5] and relaxation of lateral ellipsoidal asymmetry in the latter.[18]

ACKNOWLEDGMENT

We are grateful to P.C. Taylor and R. Zallen for helpful discussions.

[1]J. C. Phillips, J. Non-Cryst. Solids 34, 153 (1979).
[2]A. A. Vaipolin and E. A. Porai-Koshits, Fiz. Tverd. Tela 2, 1656 (1960) [Sov. Phys.–Solid State 2, 1500 (1960)]; 5, 246 (1963) [5, 178 (1963)].
[3]J. C. Phillips, J. Non-Cryst. Solids (to be published).
[4]O. Uemura, Y. Sagara, D. Muno, and T. Satow, J. Non-Cryst. Solids 30, 155 (1978).
[5]P. M. Bridenbaugh, G. P. Espinsoa, J. E. Griffiths, J. C. Phillips, and J. P. Remeika, R. J. Nemanich and S. A. Solin, Solid State Commun. 21, 273 (1977).
[6]J. Chang and R. B. Dove, J. Non-Cryst. Solids 16, 72 (1974).
[7]A. L. Renninger and B. L. Averbach, Acta Crystallogr. Sect. B 29, 1583 (1973). The attention of the reader is drawn to two points. (1) These authors use a monoclinic unit cell with $\beta=109°$, whereas Fig. 2 is drawn with a different choice of unit cell, following F. Hulliger, in *Structural Chemistry of Layer-Type Phases*, edited by F. Levy (Reidel, Boston, 1976). (2) There is apparently a misprint in Table 2 of Renninger and Averbach. The sign of x(Se(3)) should be negative.
[8]G. Dittmar and H. Schafer, Acta Crystallogr. Sect. B 32, 1188, 2726 (1976).
[9]L. Pauling, *Nature of the Chemical Bond* (Cornell University Press, Ithaca, 1960), p. 261.
[10]J. C. Phillips, *Bonds and Bands in Semiconductors* (Academic, New York, 1973), pp. 93–4.
[11]A. C. Wright and A. J. Leadbetter, Phys. Chem. Glasses 17, 122 (1976).
[12]J. C. Phillips, J. Phys. Chem. Solids 35, 1205 (1974).
[13]J. C. Phillips, J. Electrochem. Soc. 123, 934 (1976).
[14]T. Takahashi, O. Yamamoto, S. Yamada, and S. Hayashi, J. Electrochem. Soc. (to be published); S. Geller, J. R. Akridge, and S. A. Wilber, Phys. Rev. B 19, 5396 (1979).
[15]B. A. Smith, N. Cowlam, and A. M. Shamah, Philos. Mag. 39B, 111 (1979).
[16]R. Zallen, M. L. Slade, and A. T. Ward, Phys. Rev. 3B, 4257 (1971); R. Zallen and M. Slade, Phys. Rev. 9B, 1627 (1974).
[17]R. J. Nemanich, Phys. Rev. B 16, 1655 (1977).
[18]J. Szeftel and H. Alloul, Phys. Rev. Lett. 42, 1691 (1979).
[19]M. Rubinstein and P. C. Taylor, Phys. Rev. B 9, 4258 (1974).
[20]It appears that the values of η in symmetrical BO_3 units range between 0.5 and 0.8 in crystalline double oxides, and between 0.0 and 0.2 in glassy double oxides. These systems are ionic, however, and asymmetrical units (mixed bridging and nonbridging oxygens) occur. See H. M. Kriz and P. J. Bray, J. Magn. Reson. 4, 76 (1971), especially Table 2.